Pathology - Research and Practice 215 (2019) 152508

Contents lists available at ScienceDirect

Pathology - Research and Practice

journal homepage: www.elsevier.com/locate/prp

Serine/threonine kinase BUB1 promotes proliferation and radio-resistance in glioblastoma

Hai Yu[a], Suojun Zhang[b], Ahmed N Ibrahim[c], Zhong Deng[a], Maode Wang[a],*

[a] *Department of Neurosurgery, The First Affiliated Hospital of Xi'an Jiaotong University, Xi'an, Shaanxi, 710061, China*
[b] *Department of Neurosurgery, Tongji Hospital, Tongji Medical College, Huazhong University of Science and Technology, Wuhan, 430073, China*
[c] *Department of Neurology, SUNY Upstate Medical University, Syracuse, NY, USA*

ARTICLE INFO

Keywords:
Glioblastoma
BUB1
Tumorigenesis
FOXM1
Radio-resistance

ABSTRACT

BUB1 (Budding uninhibited by benzimidazoles 1), a mitotic checkpoint serine/threonine kinase, has been linked in numerous cancers to pro-tumorigenic phenomena including elevation of cellular proliferation, tumor growth, metastatic potential, and poorer patient prognosis. However, the role of BUB1 in glioblastoma remains poorly investigated. In this study, clinical analyses determined significant enrichment of BUB1 in glioblastoma with direct correlation of elevated expression to poorer prognosis in glioma patients. Genetic inhibition of BUB1 in glioblastoma tumor cells via shRNA silencing diminished both proliferative ability and tumorigenicity *in vitro* and *in vivo*. Silencing of BUB1 was additionally determined to promote the cytotoxic effect of irradiation on glioblastoma tumor cells, and investigation of the underlying pathways revealed the roles of DNA mismatch repair, spliceosome and c-Myc pathways. Mechanistically, FOXM1 was determined to positively regulate transcription of BUB1 via direct promoter region binding. For validation, pharmacologic inhibition through administration of a BUB1 inhibitor demonstrated attenuated glioblastoma cellular proliferation *in vitro* as well as delayed tumor growth with prolonged survival *in vivo*. Collectively, this study demonstrates a novel therapeutic target for glioblastoma in the form of BUB1, which plays a pivotal role in GBM proliferative and radio-resistance capacities in a FOXM1-dependant manner.

1. Introduction

Glioblastoma (GBM) continues to predominate as the most frequent and lethal primary brain tumor in adults, resulting in a median survival of only 15 months [1]. Despite multi-modal approaches involving aggressive surgical resection, as well as concurrent and adjuvant chemoradiotherapy, curative efforts have broadly met little to no success owing to GBM's inherent and adaptive therapeutic resistance mechanisms. Representing one of only a few therapies that have demonstrated significant clinical efficacy, irradiation (IR) has been broadly applied in therapeutic management of GBM [2], and approximately 50% of all cancer patients will receive IR during the course of their treatment [3]. In order to combat post-IR adaptive therapeutic resistance of GBM, focus has now shifted toward the identification and development of novel therapeutic approaches targeting key evolutionary oncogenic pathways.

BUB1 (Budding uninhibited by benzimidazoles 1) is a mitotic checkpoint serine/threonine kinase that plays crucial roles in chromosome segregation [4], recruiting members of the mitotic checkpoint complex and activating the spindle checkpoint [5]. BUB1 belongs to the budding uninhibited by Benzimidazole (BUB) and the mitotic arrest deficient (MAD) gene families, including BUB1 and BUB3, and MAD1, MAD2, and MAD3 (BUBR1) [6]. These kinases aid in the premature separation of sister chromatids until all chromosomes are properly attached to kinetochores, ensuring the fidelity of chromosome segregation [7], and are known as mitotic spindle assembly checkpoint (SAC) genes [8].

BUB1 has only recently been recognized as an oncogene in tumors of diverse origins. In human gastric carcinomas, correlation has been demonstrated between BUB1 expression and tumor proliferation activity [9]. In papillary renal cell carcinoma, gene expression alternation analyses concluded BUB1 as a key prognostic biomarker [10], with a similar role reported in pancreatic ductal adenocarcinoma [11]. In basal-like breast cancer, bioinformatics analyses suggested BUB1 as one of 10 hub genes associated with tumor initiation and progression [12]. In breast cancer metastases to the brain, an investigation of hub genes revealed BUB1 as significantly associated with poorer clinical outcomes and suggested BUB1 as a potential therapeutic target [13]. In

---

* Corresponding author at: Department of Neurosurgery, The First Affiliated Hospital of Xi'an Jiaotong University, Xi'an, Shaanxi, China.
E-mail address: maodewang@163.com (M. Wang).

https://doi.org/10.1016/j.prp.2019.152508
Received 29 April 2019; Received in revised form 30 May 2019; Accepted 20 June 2019
0344-0338/

hepatocellular carcinoma, BUB1 was determined to be negatively regulated by MiR-490-5p and promoted both cancer cell proliferation and invasion [14]. Most recently, in 2019, the BUB1 gene was demonstrated as a potential contributor to glioma progression [15].

BUB1 has additionally been determined to carry significance in regard to tumor therapeutic response. In non-small cell lung cancer, BUB1 was determined to be one of the key proliferation-associated genes predictive of resistance to immune checkpoint inhibitors [16]. In breast cancer, BUB1 co-inhibition with paclitaxel or olaparib induced significant reduction of tumor size in a xenograft model [17]. Mechanistically, BUB1 reportedly promotes TGF-β signaling via interaction with TGFBI in both lung and breast cancer [18]. Furthermore, interaction with BUB1 enhanced the activity of AURKB in transgenic mice, promoting spontaneous tumor formation [19]. However, despite these studies, both the functional role and underlying regulatory mechanisms of BUB1 remains seldomly investigated, and whether BUB1 plays a role in therapeutic resistance of GBM following surgical resection is poorly understood.

In the present study, we sought to determine the relevance of BUB1 to GBM, as well as its roles in GBM development, progression and patient outcomes. BUB1 was determined to be highly expressed in GBM, with elevated expression closely associated with poor prognosis in glioma patients. Silencing of BUB1 attenuated the proliferation of GBM tumor cells and contributed to IR therapy's inhibitory effect *in vitro* and *in vivo*. Investigation of the underlying mechanism determined that BUB1 was directly regulated by the transcription factor FOXM1. Finally, validation via the application of a novel inhibitor of BUB1 significantly suppressed the growth of GBM tumor cells and tumors.

2. Material and methods

2.1. Ethics

In this study, the utilization of cell lines and experimental animals (nude and SCID mice) was approved by the Scientific Ethics Committee of Xi'an Jiaotong University, Xi'an, China. The patient samples used in this study received patient consent.

2.2. Reagents and antibodies

The following reagents were used: DMEM-F12, Fetal bovine serum (FBS), Penicillin-Streptomycin, Trypsin-EDTA (Thermo scientific). Anti-β-Actin (3700, Cell signaling, WB), anti-FOXM1 (20459S, Cell signaling, ChIP), anti-BUB1 (H00000699-D01 P, Novus Biologicals, WB), anti-rabbit IgG-Horseradish peroxidase (NA934 V), anti-mouse IgG-Horseradish peroxidase (NXA931) (GE Healthcare).

2.3. In Vitro Cell Cultures

Glioma cell lines U373, U87, U138 and U251 were provided by Xi'an Jiaotong University. Normal human astrocyte (NHA) cells were used as a control. Cell lines were cultivated in DMEM/F12 medium containing 10% FBS supplement (vol%), 1% Penicillin-Streptomycin solution and the cultural medium was changed every 4–8 days.

2.4. RNA isolation and quantitative real-time PCR

mRNA was isolated by Trizol (Thermo scientific) according to the manufacturer's protocol. cDNA was synthesized by using iScript reverse transcription supermix (Bio-Rad) according to the manufacturer's protocol. qPCR was performed on StepOnePlus thermal cycler with SYBR Select Master Mix (Thermo scientific). Cycling conditions were 95 °C for 5 min, and then 50 cycles of 95 °C for 30 s, 60 °C for 30 s and 72 °C 30 s. The primer sequences used in this study include the following: BUB1 forward:

TGGGAAAGATACATACAGTGGGT; reverse: AGGGGATGACAGGGTTCCAAT; FOXM1 forward: CGTCGGCCACTGATTCTCAAA; reverse: GGCAGGGGATCTCTTAGGTTC; GAPDH forward: GGAGCGAGATCCCTCCAAAAT; reverse: GGCTGTTGTCATACTTCTCATGG.

2.5. Western Blot

Cells were lysed on ice in RIPA buffer containing 1% protease and 1% phosphatase inhibitor cocktail (Sigma). Protein concentrations were determined by Bradford method. Equal amounts of protein lysates (10 μg/lane) were fractionated by NuPAGE Novex 4–12% Bis-Tris Protein gel and transferred to a PVDF membrane (Thermo scientific). The membrane was blocked with 5% Blotting Grade Blocker Non Fat Dry Milk (Bio-Rad) for 1 h and then incubated with corresponding primary antibody overnight and next incubated with peroxidase conjugated secondary antibodies for 1 h. Staining was visualized with Amersham ECL Western Blot System.

2.6. Cell viability assay

Viability of tumor cells was determined using AlamarBlue reagent (Thermo scientific). Cells were seeded at 1000 cells per well in a 96 well plate, after indicated period of time AlamarBlue reagent was added into each well, and 6 h later fluorescence was measured (Excitation 515–565 nm, Emission 570–610 nm) using Synergy HTX multi-mode reader (BioTek).

2.7. In vivo intracranial xenograft tumor models

6-8 week old SCID or nude mice were used. The tumor cells suspension (1×10^5 cells in 5 μl of PBS) was injected into the brains of mice. Drug treatment: orally (p.o.) twice daily with vehicle (90% polyethylene glycol 400, 10% Ethanol) or BAY 1816032 (dissolved in 10% DMSO, 90% [10% HPbetaCD in PBS, pH7.8]), 1 week after injection of tumor cells. Following the development of neuropathological symptoms, mice were sacrificed and derived brains were dissected, fixed in 4% PFA for 24 h and then transferred to 10% formalin.

2.8. Irradiation treatment

For BUB1 expression alternation experiments, 100,000 cells were seeded into a 6 well plate and treated with 0/2/6 Gy separately. 72 h later, cells were collected and proceeded to qRT-PCR or Western Blot analysis. For *in vitro* cell growth assays, cells were seeded into a 96 well plate (1000 cells per well) and treated with 8 Gy. On day 1, 3, 5 and 7, cells were tested with AlamarBlue. For *in vivo* tumor formation assays, 7 days after injection, mice were subjected to fractionated radiation at the intensity of 2 Gy for 4 consecutive days.

2.9. Lentivirus production and transduction

HEK293 FT cells were transfected with the vectors (Sigma) and two packaging plasmids (psPAX2 and pMGD2) using the CalPhos Mammalian Transfection Kit (Clontech) according to the manufacturer's protocol. GBM tumor cells were incubated with viral supernatants for 24 h in the presence of 8 μg/ml polybrene.

Sequence of used shRNA: BUB1#1: NM_004336.3-520s21c1 CCGGGCAACAACAATACAGGTTATTCTCGAGAATAACCTGTATTGTTGTTGCTTTTTG (Sigma, TRCN0000288618); BUB1#2: NM_004336.x-2991s1c1 CCGGCATGGAACTACCAGATCGATTCTCGAGAATCGATCTGGTAGTTCCATGTTTTTG (Sigma, TRCN0000010308); FOXM1: NM_021953.2-2405s1c1 CCGGGCCAATCGTTCTCTGACAGAACTCGAGTTCTGTCAGAGAACGATTGGCTTTTT (Sigma, TRCN0000015546)

2.10. Flow cytometry

For apoptosis assay cells were stained with Alexa Fluor® Annexin V/

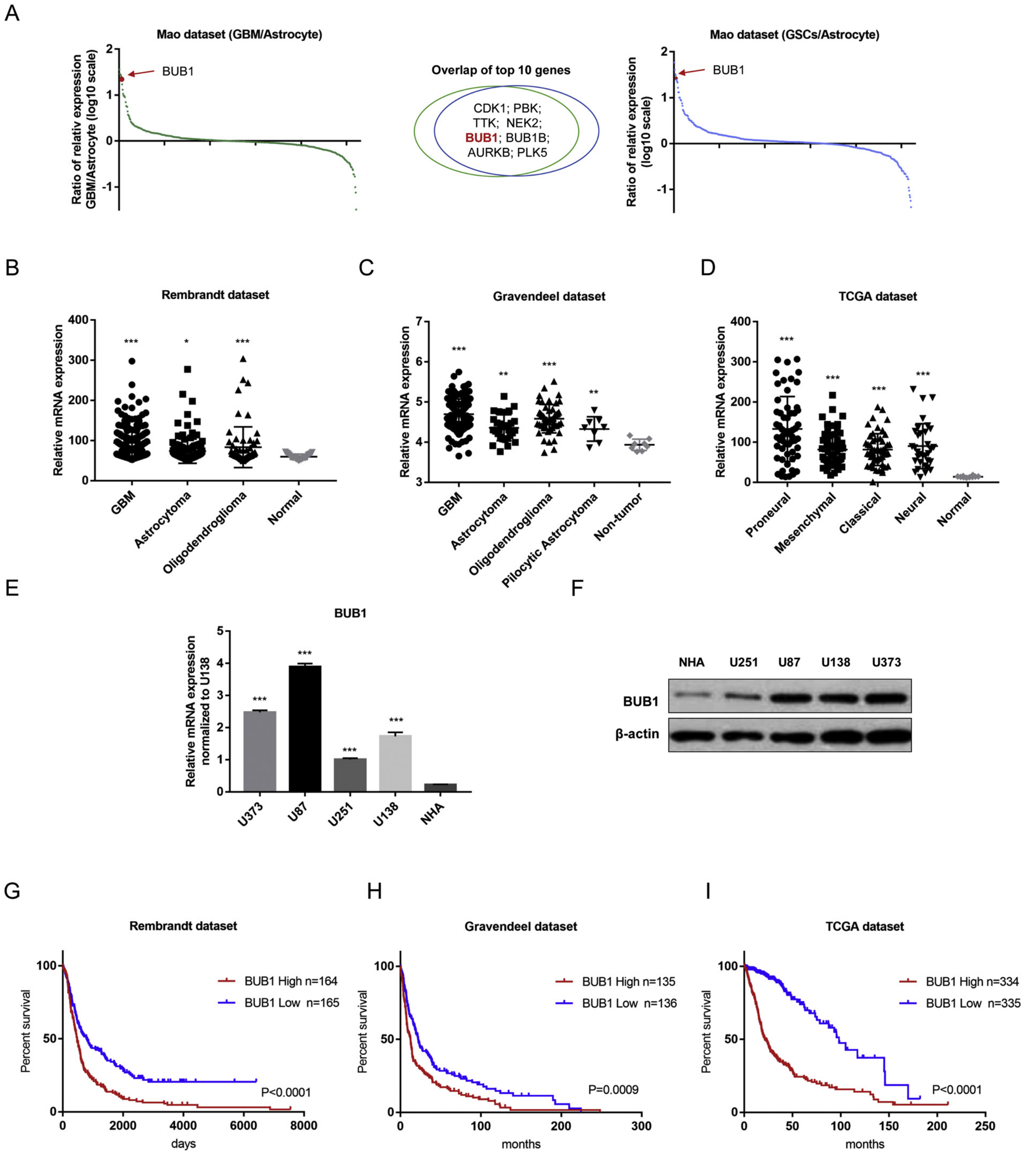

Fig. 1. BUB1 expression is enriched in GBM and is associated with poorer prognosis. (**A**) Analysis of mRNA expression of BUB1 in glioma cell lines, glioma sphere cell lines and normal human astrocyte (NHA) cell lines from indicated datasets (GSE67089). (**B, C, D**) Analysis of mRNA expression of BUB1 in Rembrandt dataset ***p < 0.001, *p < 0.05 (**B**), Gravendeel dataset ***p < 0.001; **p < 0.01 (**C**), and TCGA dataset ***p < 0.001 (**D**). (**E**) qRT-PCR comparing BUB1 mRNA expression in 4 GBM cell lines (U373, U87, U251 and U138) and a NHA cell line; ***p < 0.001; n = 3. GAPDH utilized as control. (**F**) Western Blot (WB) comparing BUB1 mRNA expression in 4 GBM cell lines (U373, U87, U251 and U138) and NHA cell line; β-actin utilized as control. (**G, H, I**) Kaplan-Meier curves comparing overall survival of glioma patients according to expression of RCC2 in indicated datasets. Log-rank test.

Dead Cell Apoptosis Kit (Thermo scientific) according to the manufacturer's protocol. After staining, samples were analyzed by Attune NxT Flow Cytometer (Thermo scientific).

2.11. BUB1 promoter luciferase assay

BUB1 promoter reporter clones (GeneCopoeia, HPRM40826) were used. U87 GBM cells were seeded in 24-well plates for 24 h, and then cells at 50–70% confluence were co-transfected with BUB1 promoter reporter plasmid, shFOXM1 and shNT plasmid as indicated by lipofectamine 3000 (Thermo scientific, L3000001) according to the manufacturer's instructions. Promoter activity assay were performed at 96 h after transfection with luciferase reporter assay kit (GeneCopoeia, LF061).

2.12. Chromatin immunoprecipitation

Chromatin Immunoprecipitation (ChIP) was performed according to

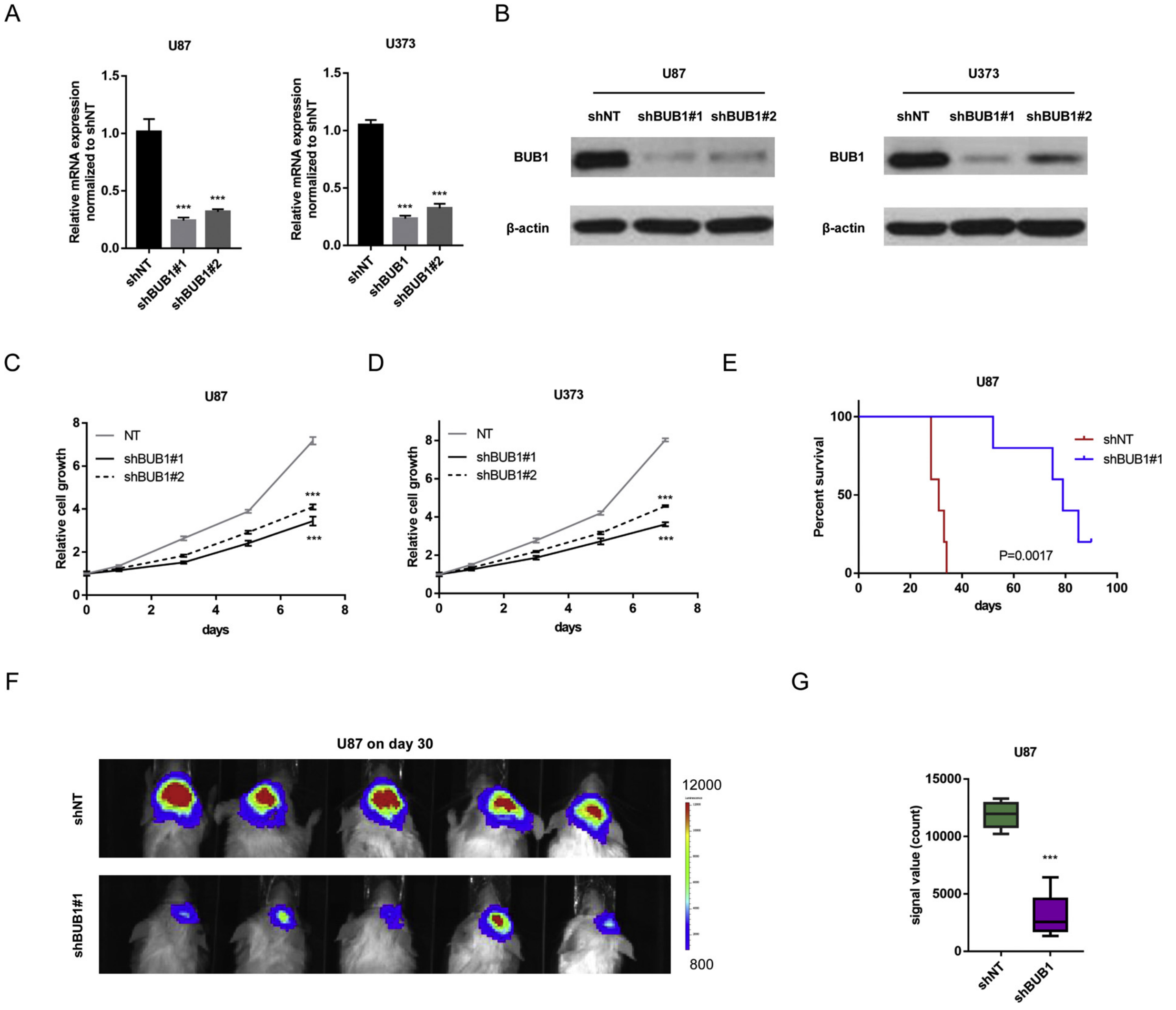

Fig. 2. Silencing BUB1 attenuates proliferation and tumorigenicity of GBM. (**A**) qRT-PCR analysis of BUB1 mRNA expression in 2 GBM cell lines (U373, U87) treated with NT-shRNA or BUB1-shRNA. ***$p < 0.001$; n = 3. GAPDH served as control. (**B**) WB for BUB1 protein expression in 2 GBM cell lines (U373, U87) treated with NT-shRNA or BUB1-shRNA. (**C**, **D**) *In vitro* cell viability assay of U87 and U373 GBM cells treated with either NT-shRNA or BUB1-shRNA. ***$p < 0.001$; n = 3. (**E**) Kaplan-Meier curve comparing overall survival of mice intracranially injected with U87 GBM cells pre-treated with either NT-shRNA or BUB1-shRNA. p = 0.0017, Log-rank test. (**F**) Bioluminescence images (BLI) of mice intracranially co-injected with luciferase-labeled U87 GBM cells pre-treated with either NT-shRNA or BUB1-shRNA on day 30. (**G**) Signal value analysis of BLI of mice intracranially co-injected with luciferase-labeled U87 GBM cells pre-treated with either NT-shRNA or BUB1-shRNA on day 30. ***$p < 0.001$.

the manufacturer's protocol. Bioruptor UCD-200 was used for sonication of DNA and 200,000 cells were applied following each reaction. Primers used: BUB1 promoter forward: AGCCGAGGACGCTGAATA; reverse: AGACTGTCGTGGCGGAAGC.

2.13. *In vivo bioluminescent imaging*

GBM tumor cells were transduced with lentiviral particles (pHAGE PGK-GFP-IRES-LUC-W) for co-expression of GFP and luciferase, and then GFP-expressing cells were sorted by FACS. Animals were administrated intraperitoneally with 2.5 mg/100ul solution of XenoLight D-luciferin (PerkinElmer) and anesthetized with isoflurane for the imaging analysis. IVIS 100 imaging system (PerkinElmer).

2.14. *Gene expression data analysis*

The data of publicly available Datasets (Obtain date: 2019.04.22) were download from http://gliovis.bioinfo.cnio.es/. Gene set Enrichment Analysis was performed using available online software (http://software.broadinstitute.org/gsea/index.jsp). Normalized values for gene expression were used as input for GSEA software. P values were calculated by permuting the genes 1000 times. During this process, the expression level of BUB1 was regarded as a phenotype. Patients (n = 669) were sub grouped into BUB1^{high} and BUB1^{low} groups. Transcriptional factor prediction was performed using available online website (http://alggen.lsi.upc.es/cgi-bin/promo_v3/promo/promoinit.cgi?dirDB = TF_8.3).

2.15. *Statistical analysis*

All data are presented as mean ± SD. Statistical differences between two groups were evaluated by two tailed t-test. Comparison among multiple groups was performed by one-way ANOVA analysis of variance followed by Dunnett's posttest. Statistical significance of Kaplan–Meier survival plot was determined by log-rank analysis. Statistical correlation was performed to calculate the regression R^2 value and Pearson's correlation coefficient. Statistical analysis was performed by Prism 6 (GraphPad Software). $p < 0.05$ was considered statistically significant.

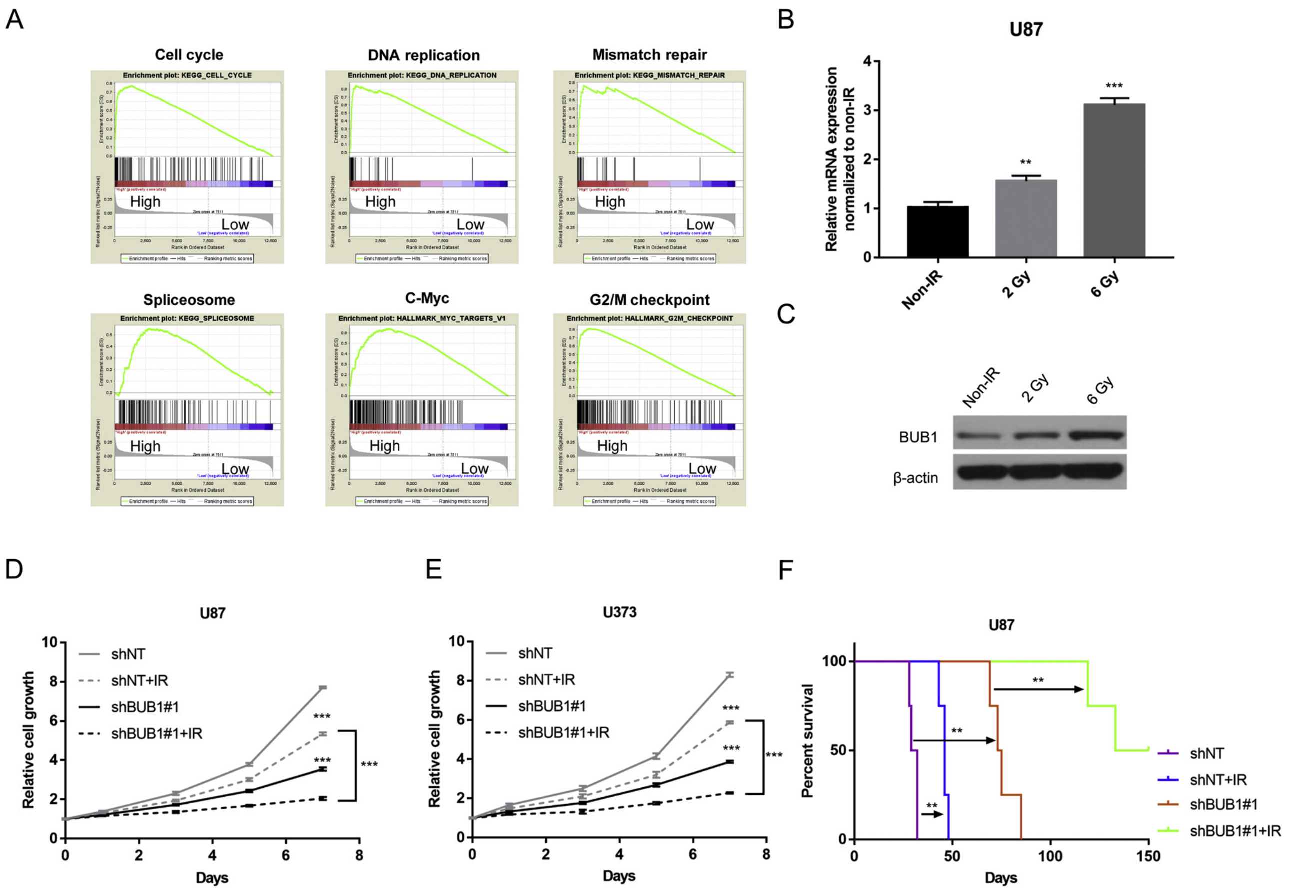

Fig. 3. Silencing BUB1 decreases radioresistance of GBM cells. (**A**) Gene set enrichment analysis (GSEA) of patient samples from TCGA dataset sub-grouped by expression of BUB1. (**B**) qRT-PCR analysis of BUB1 mRNA expression in U87 cells 72 h post-irradiation (2/6 Gy) compared to non-IR U87 cells. ***$P < 0.001$, **$P < 0.01$; n = 3. (**C**) WB for BUB1 protein expression in U87 cells 72 h post-irradiation (2/6 Gy) compared to non-IR U87 cells. (**D**, **E**) *In vitro* cell viability assay of U87 and U373 GBM cells treated with/without IR after pre-treatment with either NT-shRNA or BUB1-shRNA. ***$p < 0.001$; n = 3. (**F**) Kaplan-Meier curve comparing overall survival of mice intracranially injected with U87 GBM cells pre-treated with either NT-shRNA or BUB1-shRNA, the mice were treated with/without IR (2 Gy for 4 consecutive days). Log-rank test.

3. Results

3.1. BUB1 expression is enriched in GBM and correlates to poorer prognosis

To investigate the molecular mechanisms linking GBM tumor recurrence and therapeutic resistance, DNA microarray data (GSE67089) [20] was utilized for expression analysis of 668 kinase-encoding genes. Filtration of these genes for the top 10 highly expressed in both GBM cell lines and glioma stem-like cells (GSCs) compared to human astrocytes, revealed BUB1 (Fig. 1A). To validate the elevated expression of BUB1 in gliomas, we referred to three publicly-available datasets (Rembrandt, Gravendeel and TCGA) for analysis of BUB1 mRNA levels. BUB1 expression was significantly elevated in gliomas compared to normal brain tissue, with highest expression attributed to GBM (Fig. 1**B and C**). Additionally, BUB1 expression was significantly elevated in all four molecular subtypes of GBM (classical, mesenchymal, neural and proneural (PN)), with greatest expression in PN (Fig. 1D). For further validation, a comparison of the expression of BUB1 between GBM cell lines (U373, U87, U251, U138) and a normal human astrocyte cell line (NHA) via real-time quantitative PCR (qRT-PCR) and Western blot (WB) determined that BUB1 was highly expressed in these GBM cells (Fig. 1**E and F**). For evaluation of clinical relevance, the overall survival of glioma patients was stratified from three datasets according to tumor expression of BUB1. Analysis revealed that high-BUB1 expression leads to significantly poorer outcomes compared to their low-BUB1 counterparts (Fig. 1**G, H and I**). Collectively, these data indicate that BUB1 is preferentially expressed in gliomas and is associated with significantly poorer survival of glioma patients.

3.2. Silencing BUB1 attenuates GBM proliferative and tumorigenic capacities

Next, we sought to examine the biological role of BUB1 in GBM tumorigenesis. U87 and U373 GBM cells were infected with either non-targeting control (shNT) or shBUB1 (#1, #2) lentiviruses. The efficacy of silencing was evaluated via qRT-PCR and WB, which indicated significantly reduced expression of BUB1 on both the mRNA and protein levels in the shBUB1 group, with relatively higher silencing efficacy in shBUB1#1 (Fig. 2**A and B**). The rate of proliferation of GBM tumor cells was attenuated by BUB1 silencing when compared to the shNT group *in vitro* (Fig. 2**C and D**). For validation *in vivo*, shNT or shBUB1 U87 tumor cells were intracranially injected in SCID mice. Significantly prolonged survival was observed in the shBUB1 group (Fig. 2E), which was further corroborated by diminished signals in bioluminescence imaging (BLI) (Fig. 2**F and G**). These data indicate that BUB1 is essential to GBM cell proliferation *in vitro* and tumor formation *in vivo*.

3.3. Silencing BUB1 attenuates IR-resistance of GBM cells

Given the reliance on IR for therapeutic management of GBM following surgical resection [1], we investigated whether BUB1 is associated with IR-resistance in GBM. Gene set enrichment analysis (GSEA) was utilized for analysis of pathway alterations in BUB1-high and BUB1-low patient samples from TCGA dataset ($\text{BUB1}^{\text{high}} = 334$,

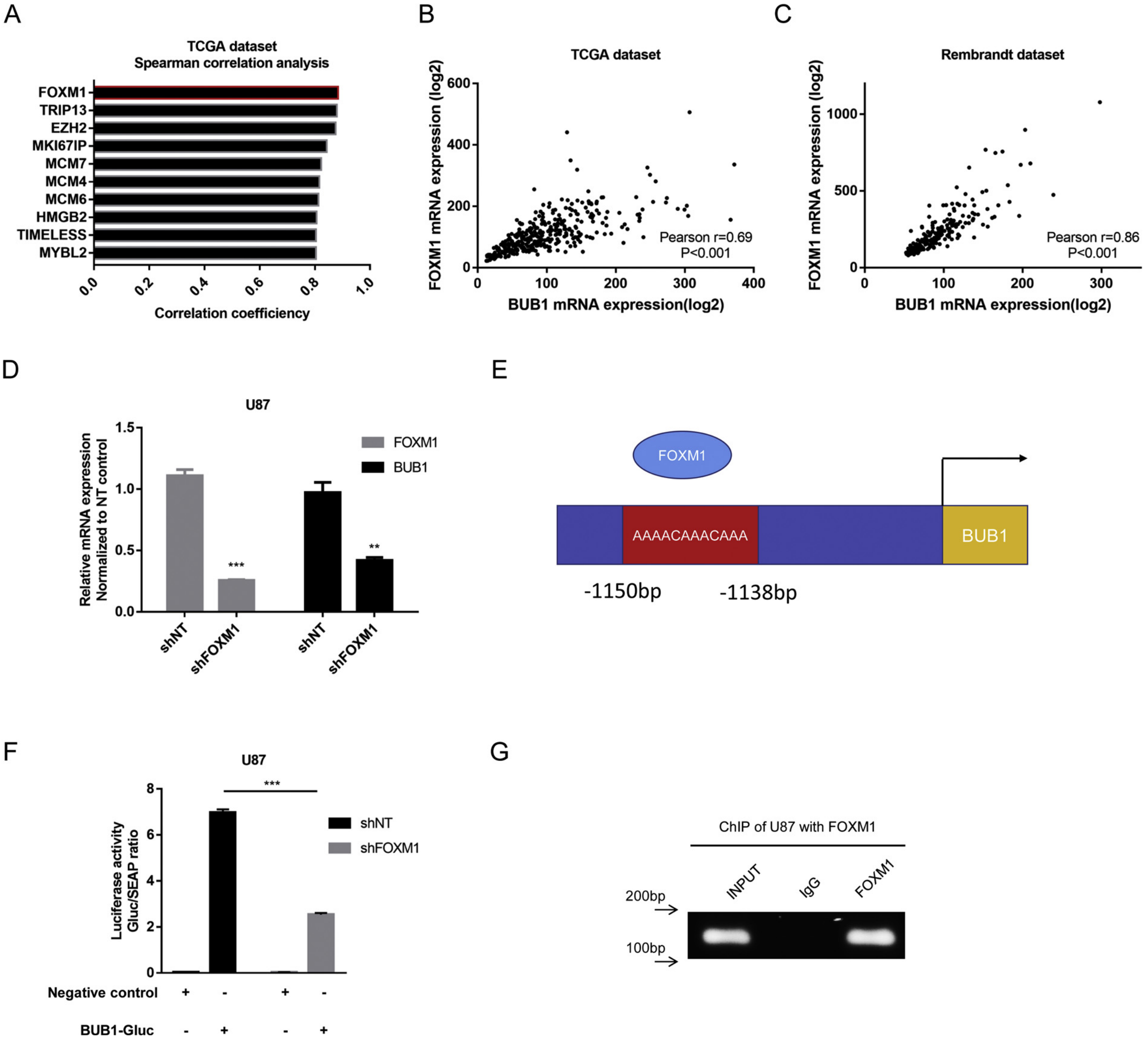

Fig. 4. BUB1 is transcriptionally regulated by FOXM1 in GBM. (**A**) Correlation analysis of BUB1 with top 10 transcription factor genes in TCGA dataset. (**B**, **C**) Correlation analysis of BUB1 with FOXM1 in TCGA and Rembrandt datasets. (**D**) qRT-PCR analysis of BUB1 and FOXM1 mRNA expression in U87 treated with either NT-shRNA or FOXM1-shRNA. **p < 0.01, *p < 0.05; n = 3. GAPDH served as control. (**E**) Schematic illustrating the binding region of human BUB1. (**F**) Luciferase activity assay of U87 GBM tumor cells co-transfected with negative control vector (containing non-promoter sequence)/BUB1-Gluc promoter reporter vector and shNT/shFOXM1 as indicated. (**G**) Representative images of RT-PCR of corresponding ChIP samples with primer for BUB1 promoter.

BUB^{low} = 335). The cell cycle, mismatch repair [2], spliceosome [21], c-Myc [22] and G2M checkpoint [2,23] pathways were enriched in the BUB1-high group, suggesting a role for BUB1 in promoting proliferation and IR-resistance in GBM (Fig. 3A). To investigate, U87 tumor cells were treated with or without 2/6 Gy IR-therapy, followed by analysis with qRT-PCR and WB after 72 h. Results indicated that BUB1 expression was significantly elevated following IR on both the mRNA and protein levels (Fig. 3**B and 3C**), suggesting a potential role for BUB1 in IR-resistance. To validate, shNT and shBUB1 U373 and U87 tumor cells were treated with IR, followed by *in vitro* growth analysis. Considerably greater cytotoxicity was observed following combined IR and shBUB1 silencing, compared with each treatment individually (Fig. 3**D and 3E**). To verify *in vivo*, the previously demonstrated intracranial xenograft model (Fig. 2) was applied. 1 week after injection of U87 tumor cells, nude mice were treated with 2 Gy IR for 4 days. Subsequent analysis of overall survival corroborated *in vitro* findings (Fig. 3F). Collectively, these data indicate that BUB1 promotes IR-resistance of GBM tumor cells.

3.4. BUB1 is transcriptionally regulated by FOXM1 in GBM

To further assess the regulatory mechanism of BUB1 expression in GBM, we referred to the TCGA dataset for correlation analysis of BUB1 with known transcription factor genes. Results indicated that FOXM1 was one of the top transcription factor genes correlated to BUB1 mRNA expression (Fig. 4**A and 4B**). Expression correlation analysis of BUB1 and FOXM1 demonstrated similar results in the Rembrandt dataset (Fig. 4C). Furthermore, silencing of FOXM1 induced significant reduction of BUB1 mRNA expression in U87 tumor cells, determined via qRT-PCR (Fig. 4D). Applying PROMO, a “virtual” laboratory for the identification of putative transcription factor binding sites (TFBS) in DNA sequences, we identified a FOXM1 binding site at the promoter area of BUB1 (Fig. 4E). To further verify, luciferase activity assay was performed on U87 cells. Results showed that silencing of FOXM1 significantly decreased transcription activity of BUB1 promoter (Fig. 4F). Finally, RT-PCR findings of chromatin immunoprecipitation (ChIP) indicated clear occupancy of FOXM1 at the BUB1 promoter region (Fig. 4G). Collectively, these data suggest FOXM1 as a potentially key regulator of BUB1 transcriptional activity in GBM tumor cells.

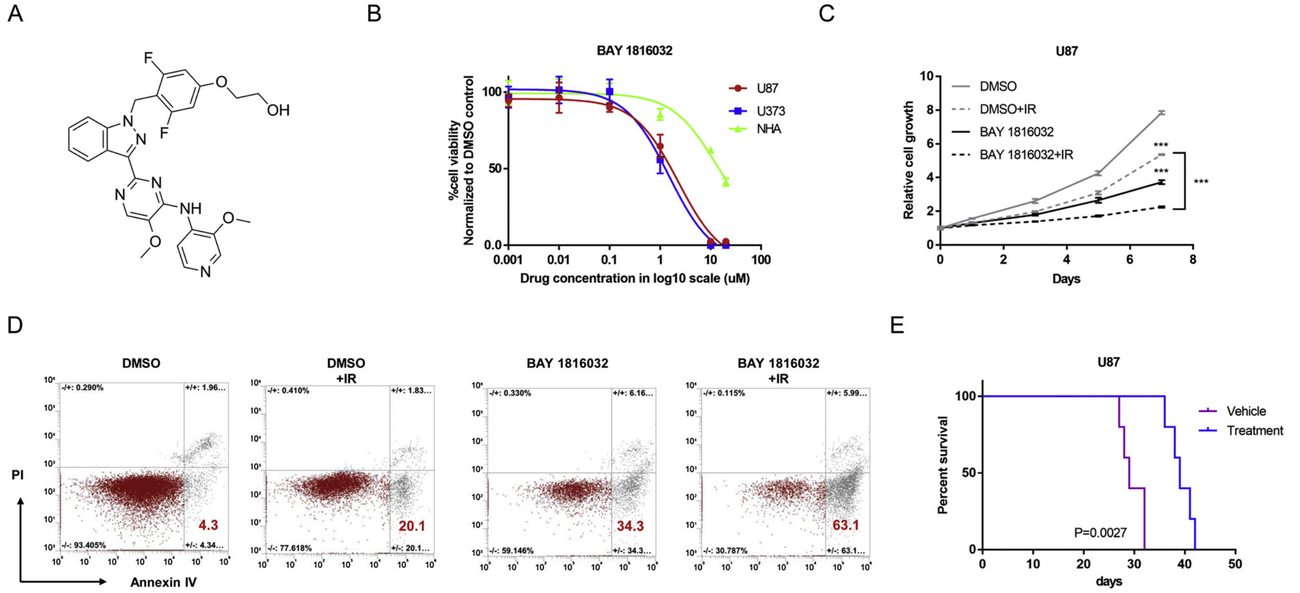

Fig. 5. Inhibition of BUB1 suppresses GBM cell growth. (**A**) Chemical structure of BAY1816032. (**B**) *In vitro* cell viability assay of U373, U87 GBM cells and NHA treated with DMSO or BAY1816032 at multiple concentrations. (**C**) *In vitro* cell viability assay of U87 GBM cells treated with/without IR after pre-treatment with either DMSO or BAY1816032. ***$p < 0.001$; n = 3. (**D**) Representative flow cytometry analysis for Annexin V/Propidium Iodide (PI) using U87 GBM cells treated with/without IR after pre-treatment with either DMSO or BAY1816032. (**E**) Kaplan-Meier curve comparing overall survival of mice intracranially injected with U87 GBM cells pre-treated with either DMSO or BAY1816032. Log-rank test.

3.5. *Inhibition of BUB1 suppresses GBM cell growth*

Finally, we sought to challenge our findings with *in vitro* and *in vivo* GBM therapeutic models. The BUB1 inhibitor, BAY1816032 [17] (Fig. 5A), was utilized for investigation of the efficacy of pharmacological BUB1 inhibition on the growth of GBM tumor cells. *In vitro* cell viability assay demonstrated relatively high sensitivity of U87 and U373 to BAY1816032 compared with NHA, with IC50 around 2 u M (Fig. 5B). *In vitro* cell growth assay demonstrated that BAY1816032 suppressed growth, with greater cytotoxicity when combined with IR compared to each individually (Fig. 5C). Next, we performed flow cytometry for apoptosis with Annexin V antibody and PI using U87 cells treated with or without 8 Gy IR in the presence of DMSO or BAY1816032. Findings determined that the percentages of cells undergoing apoptosis were markedly increased following IR when combined with BAY1816032, in comparison to IR alone (Fig. 5D). For *in vivo* validation, mice were treated with BAY1816032 (oral) or Vehicle 1 week after injection of U87 tumor cells. Significantly prolonged survival was observed in the BAY1816032 treated group (Fig. 5E). Collectively, our findings indicate that inhibition of BUB1 attenuates the tumorgenicity of GBM tumor cells, and combination of IR with BAY1816032 leads to significantly greater cytotoxicity than the individual application of either.

4. Discussion

Accumulating evidence suggests that BUB1 plays a potential role in tumorigenesis in a range of cancers including gastric carcinomas [9], renal cell carcinoma [10], pancreatic ductal adenocarcinoma [11], breast cancer [12,13,24] and hepatocellular carcinoma [14]. In this study, we demonstrated that BUB1 is significantly elevated in GBM compared to both low grade counterparts and normal human brain. In addition, survival analysis of publicly-available datasets revealed that elevated expression of BUB1 was associated with poorer prognosis of glioma patients. Silencing of BUB1 with shRNA was performed and validated, and analysis of growth of tumor cells *in vitro* and tumors *in vivo* indicated that silencing of BUB1 significantly inhibits proliferation of tumor cells and tumor development. Additionally, IR in combination with genetic silencing of BUB1 demonstrated greater cytotoxicity than each individually. Finally, validation through pharmacological inhibition demonstrated significantly diminished tumor growth with prolongation of murine mouse model survival, suggesting a role for BUB1 inhibition as a novel therapeutic modality in GBM.

Adaptive IR-resistance represents a major cause of poor clinical outcome following tumor recurrence in GBM. Previously, the role of BUB1 in IR-resistance was poorly understood. Here, our findings indicate that inhibition of cellular proliferation and tumor formation ability of GBM tumor cells by IR in the presence of BUB1 genetic silencing or pharmacologic inhibition was greater than IR alone, both *in vitro* and *in vivo*. Utilizing the TCGA dataset, GSEA identified multiple oncogene pathways associated with radio-resistance (DNA mismatch repair [2], spliceosome [21], c-Myc [22] and G2/M checkpoint [2,23]) enriched in BUB1-high expression patient samples, which is in accordance with our functional results. In addition, we validated the role of BUB1 in promoting IR-resistance via *in vitro* growth assay, and pharmacological BUB1 inhibition showed similar result. Furthermore, we observed high positive correlation for BUB1 with FOXM1 and EZH2 (Fig. 4A), two key genes previously identified as IR-resistance associated genes in GBM [25,26]. Given these findings, BUB1 likely acts as a downstream target of FOXM1 or EZH2 and plays a role in promoting IR-resistance of GBM. Additional functional confirmation will be required for validation of this hypothesis. Moreover, the downstream substrates of BUB1 in GBM remain unexplored, which warrants further study via RNA sequencing, immunoprecipitation and mass spectrum analysis.

For the underlying mechanism of regulation of BUB1 in GBM, we first analyzed the expression correlation of BUB1 with known transcription factor genes in TCGA dataset, which determined that FOXM1 was highly correlated with BUB1. Silencing of FOXM1 confirmed the positive transcriptional regulation of BUB1 by FOXM1. Previously, FOXM1 was reported to form a complex with MELK and directly regulate transcriptional expression of EZH2 in GBM [25]. Here, we identified one binding site of FOXM1 at the promoter area of BUB1 and validated the finding with ChIP-PCR, elucidating the role of FOXM1 in directly activating transcription of BUB1. However, the role of cooperative factors, such as MELK, in regulating BUB1 transcription activity remain unknown and will require further investigation.

Of note, the PN subtype was previously recognized as the predominant signature of infiltrating edge GBM tissues, which contribute to recurrence following surgical resection [27]. In this study, BUB1, FOXM1 and EZH2 demonstrated higher expression in the PN subtype compared with other subtypes in the TCGA dataset (FOXM1 and EZH2 not shown), suggesting targeting FOXM1-BUB1 interaction as a potential therapeutic modality for GBM patients that undergo surgical resection via targeting the residual edge tumor cells. To apply to clinical scenarios, we assessed the efficacy of pharmacological BUB1 inhibition on the proliferation and tumorigenicity of GBM tumor cells along with IR treatment. Our results consistently demonstrated that GBM cells are highly sensitive to BAY1816032 and confirmed decreased tumorigenesis GBM cells when treated with IR in combination with BAY1816032, indicating that inhibition of BUB1 with BAY1816032 may prove an effective therapeutic strategy for management of *de novo* and post-resection GBM.

In conclusion, our findings indicate that BUB1 is preferentially expressed in GBM and confers aggressiveness to GBM cells, and suggest BUB1 as a valuable biomarker for GBM patient outcomes. Both functional and bioinformatics analyses confirmed the role of BUB1 in promoting proliferative ability and IR-resistance in GBM. FOXM1 was identified as a key transcriptional regulator of BUB1, and inhibition of BUB1 in combination with IR attenuated tumor progression to a greater degree than each individually. Collectively, this study suggests a role for BUB1 inhibition as a potentially novel therapeutic modality in GBM.

Declaration of Competing Interest

The authors declare no conflict of interest.

Acknowledgements

We thank all the members that contributed to the study. This study was supported by The Fundamental Research Funds of Xi'an Jiaotong University; National Natural Science Foundation of China (grant no. 81802502).

References

[1] R. Stupp, W.P. Mason, M.J. van den Bent, M. Weller, B. Fisher, M.J. Taphoorn, K. Belanger, A.A. Brandes, C. Marosi, U. Bogdahn, J. Curschmann, R.C. Janzer, S.K. Ludwin, T. Gorlia, A. Allgeier, D. Lacombe, J.G. Cairncross, E. Eisenhauer, R.O. Mirimanoff, Radiotherapy plus concomitant and adjuvant temozolomide for glioblastoma, N. Engl. J. Med. 352 (2005) 987–996.

[2] S. Bao, Q. Wu, R.E. McLendon, Y. Hao, Q. Shi, A.B. Hjelmeland, M.W. Dewhirst, D.D. Bigner, J.N. Rich, Glioma stem cells promote radioresistance by preferential activation of the DNA damage response, Nature 444 (2006) 756–760.

[3] A.C. Begg, F.A. Stewart, C. Vens, Strategies to improve radiotherapy with targeted drugs. Nature reviews, Cancer 11 (2011) 239–253.

[4] P. Bernard, K. Hardwick, J.P. Javerzat, Fission yeast bub1 is a mitotic centromere protein essential for the spindle checkpoint and the preservation of correct ploidy through mitosis, J. Cell Biol. 143 (1998) 1775–1787.

[5] H. Sharp-Baker, R.H. Chen, Spindle checkpoint protein Bub1 is required for kinetochore localization of Mad1, Mad2, Bub3, and CENP-E, independently of its kinase activity, J. Cell Biol. 153 (2001) 1239–1250.

[6] M.A. Hoyt, L. Totis, B.T. Roberts, S. Cerevisiae genes required for cell cycle arrest in response to loss of microtubule function, Cell 66 (1991) 507–517.

[7] G.J. Kops, B.A. Weaver, D.W. Cleveland, On the road to cancer: aneuploidy and the mitotic checkpoint. Nature reviews, Cancer 5 (2005) 773–785.

[8] A. Musacchio, E.D. Salmon, The spindle-assembly checkpoint in space and time. Nature reviews, Molecular cell biology 8 (2007) 379–393.

[9] H. Shigeishi, N. Oue, H. Kuniyasu, A. Wakikawa, H. Yokozaki, T. Ishikawa, W. Yasui, Expression of Bub1 gene correlates with tumor proliferating activity in human gastric carcinomas, Pathobiology 69 (2001) 24–29.

[10] Z. Gao, D. Zhang, Y. Duan, L. Yan, Y. Fan, Z. Fang, Z. Liu, A five-gene signature predicts overall survival of patients with papillary renal cell carcinoma, PLoS One 14 (2019) e0211491.

[11] J. Piao, L. Zhu, J. Sun, N. Li, B. Dong, Y. Yang, L. Chen, High expression of CDK1 and BUB1 predicts poor prognosis of pancreatic ductal adenocarcinoma, Gene 701 (2019) 15–22.

[12] K. Yang, J. Gao, M. Luo, Identification of key pathways and hub genes in basal-like breast cancer using bioinformatics analysis, Onco. Ther. 12 (2019) 1319–1331.

[13] D. Tang, X. Zhao, L. Zhang, Z. Wang, C. Wang, Identification of hub genes to regulate breast cancer metastasis to brain by bioinformatics analyses, J. Cell. Biochem. 120 (2019) 9522–9531.

[14] B. Xu, T. Xu, H. Liu, Q. Min, S. Wang, Q. Song, MiR-490-5p suppresses cell proliferation and invasion by targeting BUB1 in hepatocellular carcinoma cells, Pharmacology 100 (2017) 269–282.

[15] S. Yang, K. Gao, W. Li, Identification of hub genes and pathways in glioblastoma by bioinformatics analysis, Oncol. Lett. 17 (2019) 1035–1041.

[16] S. Pabla, J.M. Conroy, M.K. Nesline, S.T. Glenn, A. Papanicolau-Sengos, B. Burgher, J. Hagen, V. Giamo, J. Andreas, F.L. Lenzo, W. Yirong, G.K. Dy, E. Yau, A. Early, H. Chen, W. Bshara, K.G. Madden, K. Shirai, K. Dragnev, L.J. Tafe, D. Marin, J. Zhu, J. Clarke, M. Labriola, S. McCall, T. Zhang, M. Zibelman, P. Ghatalia, I. Araujo-Fernandez, A. Singavi, B. George, A.C. MacKinnon, J. Thompson, R. Singh, R. Jacob, L. Dressler, M. Steciuk, O. Binns, D. Kasuganti, N. Shah, M. Ernstoff, K. Odunsi, R. Kurzrock, M. Gardner, L. Galluzzi, C. Morrison, Proliferative potential and resistance to immune checkpoint blockade in lung cancer patients, J. Immunother. Cancer 7 (2019) 27.

[17] G. Siemeister, A. Mengel, A.E. Fernandez-Montalvan, W. Bone, J. Schroder, S. Zitzmann-Kolbe, H. Briem, S. Prechtl, S.J. Holton, U. Monning, O. von Ahsen, S. Johanssen, A. Cleve, V. Putter, M. Hitchcock, F. von Nussbaum, M. Brands, K. Ziegelbauer, D. Mumberg, Inhibition of BUB1 kinase by BAY 1816032 sensitizes tumor cells toward taxanes, ATR, and PARP inhibitors in vitro and in vivo, Clin. Cancer Res. 25 (2019) 1404–1414.

[18] S. Nyati, K. Schinske-Sebolt, S. Pitchiaya, K. Chekhovskiy, A. Chator, N. Chaudhry, J. Dosch, M.E. Van Dort, S. Varambally, C. Kumar-Sinha, M.K. Nyati, D. Ray, N.G. Walter, H. Yu, B.D. Ross, A. Rehemtulla, The kinase activity of the Ser/Thr kinase BUB1 promotes TGF-beta signaling, Sci. Signal. 8 (2015) ra1.

[19] R.M. Ricke, K.B. Jeganathan, J.M. van Deursen, Bub1 overexpression induces aneuploidy and tumor formation through Aurora B kinase hyperactivation, J. Cell Biol. 193 (2011) 1049–1064.

[20] P. Mao, K. Joshi, J. Li, S.H. Kim, P. Li, L. Santana-Santos, S. Luthra, U.R. Chandran, P.V. Benos, L. Smith, M. Wang, B. Hu, S.Y. Cheng, R.W. Sobol, I. Nakano, Mesenchymal glioma stem cells are maintained by activated glycolytic metabolism involving aldehyde dehydrogenase 1A3, Proc. Natl. Acad. Sci. U.S.A. 110 (2013) 8644–8649.

[21] M.S. Pavlyukov, H. Yu, S. Bastola, M. Minata, V.O. Shender, Y. Lee, S. Zhang, J. Wang, S. Komarova, J. Wang, S. Yamaguchi, H.A. Alsheikh, J. Shi, D. Chen, A. Mohyeldin, S.H. Kim, Y.J. Shin, K. Anufrieva, E.G. Evtushenko, N.V. Antipova, G.P. Arapidi, V. Govorun, N.B. Pestov, M.I. Shakhparonov, L.J. Lee, D.H. Nam, I. Nakano, Apoptotic cell-derived extracellular vesicles promote malignancy of glioblastoma via intercellular transfer of splicing factors, Cancer Cell 34 (2018) 119–135 e110.

[22] W.J. Wang, S.P. Wu, J.B. Liu, Y.S. Shi, X. Huang, Q.B. Zhang, K.T. Yao, MYC regulation of CHK1 and CHK2 promotes radioresistance in a stem cell-like population of nasopharyngeal carcinoma cells, Cancer Res. 73 (2013) 1219–1231.

[23] S.H. Kimura, M. Ikawa, A. Ito, M. Okabe, H. Nojima, Cyclin G1 is involved in G2/M arrest in response to DNA damage and in growth control after damage recovery, Oncogene 20 (2001) 3290–3300.

[24] J.Y. Han, Y.K. Han, G.Y. Park, S.D. Kim, C.G. Lee, Bub1 is required for maintaining cancer stem cells in breast cancer cell lines, Sci. Rep. 5 (2015) 15993.

[25] S.H. Kim, K. Joshi, R. Ezhilarasan, T.R. Myers, J. Siu, C. Gu, M. Nakano-Okuno, D. Taylor, M. Minata, E.P. Sulman, J. Lee, K.P. Bhat, A.E. Salcini, I. Nakano, EZH2 protects glioma stem cells from radiation-induced cell death in a MELK/FOXM1-dependent manner, Stem Cell Reports 4 (2015) 226–238.

[26] E. Kim, M. Kim, D.H. Woo, Y. Shin, J. Shin, N. Chang, Y.T. Oh, H. Kim, J. Rheey, I. Nakano, C. Lee, K.M. Joo, J.N. Rich, D.H. Nam, J. Lee, Phosphorylation of EZH2 activates STAT3 signaling via STAT3 methylation and promotes tumorigenicity of glioblastoma stem-like cells, Cancer Cell 23 (2013) 839–852.

[27] M. Minata, A. Audia, J. Shi, S. Lu, J. Bernstock, M.S. Pavlyukov, A. Das, S.H. Kim, Y.J. Shin, Y. Lee, H. Koo, K. Snigdha, I. Waghmare, X. Guo, A. Mohyeldin, D. Gallego-Perez, J. Wang, D. Chen, P. Cheng, F. Mukheef, M. Contreras, J.F. Reyes, B. Vaillant, E.P. Sulman, S.Y. Cheng, J.M. Markert, B.A. Tannous, X. Lu, M. Kango-Singh, L.J. Lee, D.H. Nam, I. Nakano, K.P. Bhat, Phenotypic plasticity of invasive edge glioma stem-like cells in response to ionizing radiation, Cell Rep. 26 (2019) 1893–1905 e1897.